www.sciencemag.org/cgi/content/full/science.aac7263/DC1

Supplementary Materials for

A stable trimeric influenza hemagglutinin stem as a broadly protective immunogen

Antonietta Impagliazzo,* Fin Milder, Harmjan Kuipers, Michelle V. Wagner, Xueyong Zhu, Ryan M. B. Hoffman, Ruud van Meersbergen, Jeroen Huizingh, Patrick Wanningen, Johan Verspuij, Martijn de Man, Zhaoqing Ding, Adrian Apetri, Başak Kükrer, Eveline Sneekes-Vriese, Danuta Tomkiewicz, Nick S. Laursen, Peter S. Lee, Anna Zakrzewska, Liesbeth Dekking, Jeroen Tolboom, Lisanne Tettero, Sander van Meerten, Wenli Yu, Wouter Koudstaal, Jaap Goudsmit, Andrew B. Ward, Wim Meijberg, Ian A. Wilson,* Katarina Radošević

*Corresponding author. E-mail: aimpagli@its.jnj.com (A.I.); wilson@scripps.edu (I.A.W.)

Published 24 August 2015 on *Science* Express
DOI: 10.1126/science.aac7263

This PDF file includes:

Materials and Methods

Study Design

The overall objective of this study was to create soluble protein immunogens derived from the HA stem that retain the native conformation of this region and are able to induce broadly protective antibody responses in relevant animal models. To this end, molecules were rationally designed and selected from construct libraries. Candidates were characterized *in vitro* for bnAb binding, stability and presence of trimers by various techniques such as ELISA, PAGE, size exclusion chromatography (SEC), biolayer interferometry, hydrogen-deuterium exchange mass spectrometry, negative-stain electron microscopy and crystallography. Successful candidates were subsequently tested *in vivo* for immunogenicity and protective efficacy in murine and nonhuman primate influenza A challenge models. The quality of the immune responses was assessed by HA-specific ELISAs, bnAb CR9114 competition ELISAs, virus neutralization assays, and surrogate ADCC assays. Protective efficacy in mice was defined by survival proportion, survival duration, bodyweight loss, and clinical score. In the nonhuman primates, efficacy was defined by tracheal viral load and cumulative body temperature increase post-challenge. Sample size justification (power analysis): for the murine challenge studies, sample size was such that the three studies had at least 80% power to detect a true 62% to 75% difference in survival proportion between the vaccinated groups and the mock-immunized negative control group. For the nonhuman primate challenge study with 6 animals per group, there was 80% power to detect a treatment effect between 0.7 and 1.7 °C relative to a control group mean of 2.7 °C on the cumulative body temperature increase at day 3. For the AUC viral load in tracheal swabs by PCR, the study had 80% power to detect a treatment effect between 1.1 and 2.8 relative to a control group mean of 6.4 log10 (RNA copies/mL x day). Randomization: mice were randomly assigned to cages and cages were allocated to treatment groups. Nonhuman primates were randomly allocated to treatment groups according to a randomized block design based on the age and weight of the animals. Blinding: the study technicians were not blinded to the vaccines administered and during the clinical scoring and bodyweight measurement post-challenge. Replication: mice and monkey experiments included 10-14 and 6 animals per group, respectively, and were performed once.

Statistical analysis

For mouse challenge studies, a study was considered valid only when there was a statistically significant difference in survival proportion (Fisher's exact-test, 2-sided) between negative (mock) and positive (CR6261) challenge model control groups. Statistical differences between mini-HAs and the mock-immunized negative control group were evaluated for survival proportion, survival time, change in bodyweight and clinical score as described previously (41, 44). Survival proportion and survival time after challenge were analyzed using Fisher's exact test and log-rank test, respectively, with Bonferroni adjustment for multiple comparisons. Repeated measurements in the challenge phase (bodyweight and clinical scores) were summarized as a single outcome per animal using an area under the curve (AUC) approach where missing values for

animals that died early were imputed with a last-observation-carried-forward method. Bodyweight data are expressed as change relative to the day 0 measurement. The net AUC was then defined as the summation of the area above and below the baseline. An analysis-of-variance (ANOVA) was performed on AUCs, with group as factor and assuming variance heterogeneity between groups and followed by Bonferroni-adjusted multiple comparisons. All tests were two-sided at the 5% significance level. Survival data are presented as Kaplan Meier curves per group, bodyweight data as mean relative change from baseline with normal-based 95% CI per group per day and ordinal clinical scores as median with interquartile range per group per day.

Statistical analysis of the difference in AUC body temperature increase between treatments in the cynomolgus macaque challenge study was performed using pairwise unequal-variance two-sided t-tests at the 5% significance level with Tukey-Kramer adjustment for multiple comparisons. The viral loads in the tracheal swabs measured by PCR were summarized per animal as AUC over the 21 day post-challenge follow-up period. The log-transformed AUC values were compared between treatment groups in an analysis-of-variance followed by pairwise two-sided t-tests at the 5% significance level with Tukey adjustment for multiple comparisons. HA-specific ELISA antibody titers were log-transformed and analyzed with a likelihood-based analysis-of-variance with treatment as factor and with titers at the LOD taken as left-censored values, followed by pairwise two-sided t-tests at the 5% significance level with Tukey-Kramer adjustment for multiple comparisons.

Mini-HA rational design and screening

The mini-HA design was based on the HA sequence from A/Brisbane/59/2007 (H1N1) (ACA28844) and the crystal structure of full-length (FL) HA A/California/04/2009 (H1N1) (PDB ID 3LZG). PyMOL Molecular Graphics System, Version 1.5.0.3 (Schrödinger, LLC) was used as the molecular visualization software.

To retain and stabilize the native pre-fusion conformation of HA, the protease cleavage site was removed by a single mutation (R329Q; H3 numbering) (45) in all constructs. The constructs designed in stage I contained the HA transmembrane domain, were expressed at the surface of HEK293F cells, and were analyzed for CR9114 binding using flow cytometry. The HA head was omitted from the construct by deletion at several different positions on HA1 and replacing the deleted residues by a four glycine linker (GGGG). The construct with the HA head domain removed by deletion of HA1 residues N45-P306 exhibited the best binding to CR9114 and was selected for further modifications. To increase mini-HA solubility, several residues at the newly exposed surface, in the so-called B loop, were mutated from hydrophobic to hydrophilic (HA2 F63S, V66T and L73S) or neutral (HA2 F70G). To further stabilize the bnAb stem epitope, a disulfide bridge was engineered at position R310C (HA1) and T93C (HA2). An increase in stability of the stem construct was further achieved by replacing the N-terminal 16 residues of the long helix (from residues R75 to D90 of the CD helix) with the initial 16 of the 31 residues of the GCN4 leucine zipper sequence to aid trimerization (46, 47). Among the tested mini-HA constructs (in total 22 candidates), the best binding to CR9114 was observed with mini-HA construct #2708, which was also significantly better than the binding to previously published constructs (#2225) (48) (fig. S1A).

In the next stage (Stage II, Fig. 1A), His-tagged soluble protein constructs were generated through deletion of the transmembrane and cytoplasmic domains, expressed in a soluble form in HEK293F cells, and then purified. In total, seven different variants of soluble mini-HA were generated and tested for binding to CR9114. The best binder, mini-HA #4157 (fig. S1B), which is the soluble version of membrane-expressed #2708, was also generated in an alternative, 11 C-terminal residue longer form called mini-HA #2759 (fig. S2). We found no significant differences between these two constructs in any of the assays, and therefore used them interchangeably throughout the program.

The third design step (Stage III, Fig. 1A) was aimed at further improving the structural integrity of the bnAbs epitopes, in particular the CR6261 epitope, while retaining good expression. We implemented a knowledge-based, semi-rational library approach, using mini-HA #4157 as the starting point. Nine residues with exposed hydrophobic side-chains that potentially could affect protein stability and solubility were selected for implementing sequence variation: five residues in the B loop (HA2: M59, F63, V66, F70 and L73) and four in the uncleaved fusion peptide loop (HA1: I323 and I326; HA2: F9 and I10). To restrict the total library size, we limited the diversity of residues to be introduced, yielding a yeast library of $2.8x10^6$ variants. Screening approximately 27.000 library clones, which were produced in *Pichia pastoris*, for binding with CR6261 and for expression yield resulted in 289 clones with improved binding to CR6261 as well as comparable binding to CR9114. Twenty four of the highest scoring clones were expressed in HEK293F cells (fig. S1C), and five of these were purified. Mini-HA #4454 (with six mutations I323K, I326K, I10T, S63Y, T66I and G70Y; figs. S1C and S2) exhibited the most favorable attributes in terms of protein expression, solubility and bnAb binding.

In the next steps, we focused on designing features to promote and stabilize the trimeric conformation of mini-HA. In Stage IV (Fig. 1A), we tested the effect of modifying the position of the inserted GCN4 motif on epitope conformation and protein expression. By shifting the GCN4 motif one residue upstream or downstream in the sequence of ten best library candidates, we generated 22 candidates, which were then screened for binding with CR6261, as well as for the presence of oligomeric species (i.e. dimers, trimers), using a CR9114 sandwich (multimer) ELISA. The best candidate from this stage, mini-HA #4650 (fig. S2), with the GCN4 sequence at residue HA2 R76 to D90 of the CD helix, exhibited improved binding with CR6261 compared to its precursor mini-HA #4454 (fig. S1D), and demonstrated a propensity for oligomerization (fig. S1E).

In the final stage (Stage V, Fig. 1A), we aimed to promote and stabilize the trimeric configuration in a covalent manner by introducing intermolecular cysteine bridges. Twelve different intermolecular cysteine bridges were introduced on two candidates from stage IV that showed the strongest propensity to oligomerize, generating 24 constructs for further testing. Mini-HA #4900 (fig. S2), which is based on mini-HA #4650 with a cysteine bridge at position K68C (HA2) on the B loop and R76C (HA2) on the CD helix, exhibited the strongest oligomerization propensity in a CR9114 sandwich (multimer) ELISA (fig. S1E). An alignment of the lead constructs for each stage is depicted in fig. S1F.

FACS screening of membrane-associated mini-HA variants

Constructs encoding mini-HAs containing transmembrane and cytoplasmic domains were transfected using 239FectinTM Reagent solution (Invitrogen) and expressed transiently on the surface of Human Embryonic Kidney (HEK) 293F cells cultured in FreestyleTM medium. On day 3 post-transfection, the cells were transferred to a 96-well plate, centrifuged and washed three times with phosphate buffered saline (PBS) containing 1% bovine serum albumin (BSA). The primary antibodies CR6261, CR9114, CR8020, and the polyclonal anti-H1 A/California/04/2009 (Sino Biological) antibody were added to the cells at a final concentration of 1.5 μg/ml for the bnAbs and 34 μg/ml for the polyclonal antibody. Following incubation for 1 hour at 4 °C with primary antibody, the cells were washed three times with PBS/1% BSA. Next, the fluorescently labeled secondary antibody, PE labeled goat anti-human IgG (SouthernBiotech) or goat anti-rabbit IgG (Thermo Scientific), in PBS/1% BSA was added to a final concentration of 2.5 μg/ml and 6.6 μg/ml, respectively. After incubation for 1 hour at 4 °C with the secondary antibody, the cells were washed three times using PBS/1% BSA followed by addition of viability indicator TO-PRO3 (Invitrogen) to exclude dead cells in FACS analysis. Samples were subsequently analyzed in a FACS LSR Fortessa (BD Biosciences).

Library screening

DNA sequences encoding the library constructs were transformed into *Pichia pastoris*. To express soluble proteins, the HA leader sequence was replaced with the yeast alpha factor leader sequence. A C-terminal sequence, containing a FLAG-tag, foldon trimerization domain and His-tag, was added for detection and purification purposes. Binding of bnAbs CR6261, CR9114 and CR8020 (negative control) to library variants was determined by ELISA. Briefly, ELISA plates were coated with a 2 μg/ml bnAb solution (20 μl/well) at 4 ^{o}C overnight, blocked with 4% non-fat dry milk in PBS for a minimum of 1 hour at room temperature (RT). After washing the plates, 20 μl of cell culture medium (neat or diluted) was added to each well and incubated for at least 1 hour at room temperature (RT). The ELISA plates were then washed and 20 μl of anti-FLAG/HRP antibody solution (Sigma A8952, diluted 20000 times in 4% non-fat dry milk in PBS-Tween) was added. After incubation (1 hour at RT), plates were washed once, and 20 μl luminescent substrate (Thermoscientific C#34078) was added. Alternatively, a colorimetric detection method was used to develop the signal.

Expression of library variants was determined from a homogeneous, time-resolved fluorescence (HTRF) assay (for a general description see 49). To this end, a mixture of Terbium (TB)-labeled anti-FLAG monoclonal antibody (donor) and Alexa488-labeled anti-His monoclonal antibody (acceptor) (HTRF solution) was prepared by adding 210.5 μl Anti-FLAG-TB (stock solution 26 μg/ml) and 1.68 ml of anti-HIS-Alexa488 (stock solution 50 μg/ml) to 80 ml of a 1:1 mixture of culture medium and 50 mM HEPES + 0.1% BSA. HTRF solution (19 μl) was added to each well of an ELISA plate and 1 μl of culture medium was added. After excitation followed by a delay to allow interfering short-lived background signals to decay, the ratio of fluorescence emission at 520 nm and 665 nm was determined. As this signal is dependent only on the close proximity of FLAG-tags and His-tags and does not require proper folding of the H1 mini-HA, it is a

measure of total protein content in the sample and can be used to normalize the mAb binding signals of different library variants.

To screen the individual library clones, yeast colonies were cultured in 96-well plates for 3 days and the culture medium was collected. A primary binding screen was performed on the undiluted culture medium using coated CR6261 as the capture antibody and anti-FLAG conjugated to HRP for detection purposes. Total protein content was determined at 20-fold media dilution using the HTRF assay described above. Clones with an improved ratio of CR6261 binding to HTRF signal (higher than mean + 2SD) compared to the ratio for the parent construct were selected. For the selected clones, CR6261 and CR9114 binding was confirmed by ELISA using a 4-point titration (1:5 dilution series); only those clones with improved CR6261 binding (defined as above) were selected. CR9114 binding was found to be in agreement with CR6261 binding for all clones; i.e. clones with improved CR6261 binding also exhibited improved responses in CR9114 binding and vice versa. Finally, all confirmed library hits were ranked based on their CR6261 binding signal after normalizing to level of protein expression as measured by HTRF. A set of 24 hits with the highest CR6261 binding signals were expressed in mammalian cells (HEK293F) to confirm increased CR6261 binding.

Production and purification of soluble mini-HAs and FL HA

The mini-HA proteins were produced in HEK293F cells cultured in Freestyle™ medium by transient transfection using 293fectin™ transfection reagent (Invitrogen) of the plasmid pcDNA2004 (pcDNA3 vector with an enhanced CMV promoter) containing the genes encoding mini-HA variants. Culture supernatants were harvested at day 7 by centrifugation followed by filtration over a 0.2 μm bottle top filter (Corning). All proteins were purified in a two-step protocol using an ÄKTA Avant 25 system (GE Healthcare Life Sciences). First, immobilized metal affinity chromatography was applied, using either pre-packed His Trap HP column or self-packed HiScale 26/20 column with Ni Sepharose HP (GE Healthcare Life Sciences), depending on the scale and expected yield of the preparation. The bound proteins were eluted by stepwise gradients to 100 mM and 300 mM imidazole in buffer. Elution fractions were pooled and the buffer was exchanged to PBS or TRIS buffer (20 mM TRIS, 150 mM NaCl, pH 7.8) by running a HiPrep 26/10 desalting column (GE Healthcare Life Sciences). Next, the collected fractions were purified by size exclusion chromatography using a HiLoad 16/60 or HiLoad 26/60 Superdex-200 prep grade column (GE Healthcare Life Sciences). The peak fractions were analyzed on SDS and native polyacrylamide gel electrophoresis, pooled and concentrated by centrifugation using centrifugal filter amicon units Ultra-15 ultracel 10,000 NMWL (Millipore). The yields of mini-HA constructs purified from 5 x 300 ml cultures were 10–21 mg/L.

Binding of Fab fragments of CR6261 and CR9114 to soluble mini-HA proteins

In-solution binding of Fab fragments to the mini-HA proteins was monitored by size exclusion chromatography (SEC) and multi-angle light scattering (MALS) analysis using a high-performance liquid chromatography system (Agilent Technologies) and miniDAWN TREOS (Wyatt) instrument coupled to a Optilab T-rEX Refractive Index Detector (Wyatt). In total, 40 μg of soluble mini-HA or Fab fragments of CR6261,

CR9114 and CR8020 (negative control) were applied to a TSK-Gel G3000SWxl column (Tosoh Bioscience) equilibrated in running buffer (150 mM NaPi, 50 mM NaCl, pH 7.0). Complex formation was verified by analysis of soluble mini-HA incubated in the presence of a 1.2-fold molar excess of Fab fragments. The data were analyzed by the Astra 6 software package and molecular weight calculations were derived from the refractive index signal.

Binding of CR6261 and CR9114 to soluble FL HA and mini-HA proteins

The avidity of bnAbs CR6261 and CR9114 binding to the soluble FL HA and mini-HA proteins was assessed by biolayer interferometry (Octet) measurements (ForteBio). Biotinylated antibodies were immobilized on Streptavidin (SA) Dip and Read biosensors for kinetics (ForteBio). Real-time binding curves were measured by applying the sensor in a two-fold dilution series of the analyte in PBS diluted 10x concentrated kinetic buffer (ForteBio). The starting concentrations of FL HA and mini-HA proteins were in the range of 10-2000 nM, depending on the specific FL HA/mini-HA and antibody combination. Dissociation constants (K_D) were determined using steady state analysis, assuming a 1:1 binding model for bnAb to soluble FL HA and mini-HA binding.

CR9114 sandwich (multimer) ELISA

To detect the presence of oligomeric HA and mini-HA, Maxisorp 96-well plates (Nunc Thermo Fischer Scientific, Bremen, Germany) were coated with purified CR9114 diluted to 2.0 μg/ml in PBS pH 7.4 (Gibco, Life Technologies, Paisley, UK) O/N at 4 °C. Plates were washed with PBS pH 7.4 containing 0.05% Tween-20 (Calbiochem, Merck Millipore, Darmstadt, Germany) (PBS-T) and subsequently blocked with block buffer (PBS pH 7.4 containing 4% dried skimmed milk (Difco, BD, Breda, the Netherlands)) for 1.5 hour at RT. After washing with PBS-T, plates were incubated with a titrated amount of mini-HAs or FL HA diluted in block buffer for 1 hour at RT (3-fold dilution series, in duplicate, with a starting concentration of 5 μg/ml). Plates were washed with PBS-T and biotinylated CR9114 was added to the plate at 0.2 μg/ml in block buffer. Following incubation for 1 hour at RT, the plates were washed with PBS-T and a 1:500 dilution of horseradish peroxidase-labeled Streptavidin (BD Pharmingen) in block buffer was added and incubated for 1 hour at RT. Plates were washed with PBS-T and developed using OPD substrate (Thermo Fischer Scientific Pierce) in the dark. The colorimetric reaction was stopped after 10 min by adding 1M H_2SO_4. The optical density (OD) was measured at 492 nm.

Hydrogen–deuterium exchange mass spectrometry (HDX-MS)

Reagents TCEP (tris-(2-carboxyethyl) phosphine), formic acid (MS grade and ~98%), sodium phosphate monobasic, sodium phosphate di-basic and sodium chloride were purchased from Sigma-Aldrich (St. Louis, MO). Deuterium oxide (99.9%) was purchased from Cambridge Isotope Laboratories (Andover, MA). Guanidine hydrochloride (8.0 M) was purchased from Thermo Scientific (Waltham, MA). Acetonitrile and water were ULC/MS grade and purchased from BioSolve (Valkenswaard, The Netherlands). All chemicals were used without further purification unless otherwise specified.

Mini-HA protein concentrations were adjusted to 60 μM in 100 mM sodium phosphate buffer at pH 7.4. For each sample, 3 μl of protein solution was diluted 20-fold with either PBS in H_2O at pH 7.4 (for non-deuterated experiments) or PBS in D_2O at pD 7.4 (for deuterated experiments). Sixty μL aliquots of diluted samples were incubated in triplicate at 25 °C. The labeling reaction for the deuterated samples was quenched by 1:1 volume addition of ice cold quenching buffer containing 100 mM potassium phosphate, 4 M guanidine hydrochloride and 0.5 M TCEP at pH 2.5 for time intervals of 1, 10 and 60 min. Similarly, non-deuterated samples were incubated at 25 °C for 15 min prior to quenching step and used as time 0 points. After a brief vortex, the quenched samples were flash frozen in liquid nitrogen and stored at -80 °C until MS analysis.

Samples collected at different time points were injected into a Waters nano-ACQUITY UPLC system equipped with HDX technology (Waters Corporation, Milford, MA). Online digestion was performed on a immobilized pepsin column (Poroszyme Immobilized Pepsin Cartridge) at 22 °C with 0.05% formic acid in H_2O (pH 2.5) at a flow rate of 125 μl/min. Peptides were trapped and desalted online on a ACQUITY UPLC BEH C18 1.7 μm VanGuard Pre-column 3/Pk 2.1 x 5 mm (Waters) for 4 min at 0 °C. Peptide separation utilized with a 19-min linear acetonitrile-water gradient (8−95% containing 0.1% formic acid) at a flow rate of 40 μl/min using ACQUITY UPLC BEH C18 1.7 μm 1.0 x 100 mm analytical column (Waters) at 0 °C.

The eluent was directed into a Synapt G2 ESI Q-ToF MS instrument (Waters) with lock-mass correction using Leu-Enkephalin solution. The following instrument configuration was used: capillary voltage was 1.5 kV, sampling cone voltage was 30 V, trap collision voltage values were 4 V (low energy) and 20−40 V ramping (elevated energy), source temperature was 100 °C and desolvation temperature was 250 °C. Mass spectra were acquired over an m/z range of 50−2000 in positive MSE mode. To eliminate peptide carryover, two blank injections of 0.1% formic acid in H_2O were injected after each sample run. Peptides from the unlabeled sample data were identified using ProteinLynx Global Server (PLGS) 2.5.2 software (Waters). Deuterium uptake was calculated and compared to the non-deuterated, unlabeled sample using DynamX 2.0 software from Waters Corporation. Only peptides observed in both the non-deuterated and deuterated samples above the pre-set thresholds of 2000 intensity, 0.2 minimum products per amino acid, and present in 2 out of 3 replicates, were further considered. Absolute deuterium incorporation per peptide at a given time point corresponding to the centroid value across the backbone amides was determined by comparison with the non-deuterated sample at t=0. Results were averaged across triplicate analyses.

Differential scanning calorimetry (DSC)

DSC measurements were carried out using a MicroCal VP-Capillary DSC system (GE Healthcare). The thermal denaturation of mini-HA samples (concentration of monomer units 18 μM) was followed between 20 and 90 °C at a scan rate of 1 °C/min. The reversibility of the thermal transitions was checked by reheating samples after a first scan. The raw data were baseline-corrected by subtracting sham PBS temperature ramp profiles and normalized per concentration of mini-HA monomer to obtain the excess heat capacities. Data were fitted to a non two-state transition model using the Origin 7.0 (Microcal) software.

Electron microscopy and sample preparation

Samples for electron microscopy were prepared directly from SEC-eluted fractions of mini-HA constructs bound to Fab CR9114, as described below. Carbon-coated copper grids (400 mesh) were first glow-discharged with a Gatan Solaris plasma cleaner, then incubated with sample (~20 s application time at around 1 μg/mL total protein concentration) and tungstate stain (~20 s application of Nano-W, from Nanoprobes Inc.) Micrographs were acquired at 52000X magnification, at a nominal defocus of 0.7-1.5 μm, on a Tecnai Spirit (120 kV accelerating voltage). Leginon (50) was used to automate acquisition. A Tietz charge-coupled device camera was used to record 4096 x 4096 pixel micrographs at 2.05 Å/pixel. Single particles were automatically identified using a difference-of-Gaussians algorithm implemented in the Appion package (51), and were analyzed as 64x64 pixel boxes after binning by a factor of 3 (for the mini HA #4900 complexes) or 2 (for #4454 and #4650 complexes). Noisy peaks were excluded through filtering based on mean/standard deviation and manual examination of reference-free class averages derived from CL2D (52) and "topology alignment" (53) as implemented in Appion (51). Final classification used ISAC (54) as distributed with EMAN2/SPARX (55, 56) with low-pass filtering ranging from 14-30 Å. Class averages were interpreted through comparison with projections from models derived from a high-resolution structure of Fab CR9114 bound to HA (PDB ID 4FQI, (3)).

Crystallization and structural determination of mini-HAs #4454 or #4900 in complex with CR9114 Fab

His-tagged mini-HA #4454 expressed in mammalian 293F cells and CR9114 Fab (3) were mixed in a 1:1.2 molar ratio. His-tagged mini-HA #4900 expressed in baculovirus system Hi5 cells was also mixed in a 1:1.2 molar ratio with CR9114 Fab. The mixture was incubated overnight at 4 ºC before further purification by gel filtration (Superdex 200 column) to remove uncomplexed mini-HA or Fab. Crystallization experiments were set up using the sitting drop vapor diffusion method. Initial crystallization conditions were obtained from robotic crystallization trials using the automated Rigaku Crystalmation system at the Joint Center for Structural Genomics (JCSG). Following optimization, diffraction quality crystals of the #4454-CR9114 Fab complex were obtained by mixing 0.5 μl of the concentrated protein (8.5 mg/ml) in 20 mM Tris, pH 8.0, 150 mM NaCl, and 0.02% NaN_3 with 0.5 μl of a reservoir solution containing 0.1 M Tris pH 8.0, 0.2 M disodium hydrogen phosphate and 22% (w/v) PEG4000 at 22 ºC. The crystals were flash-cooled in liquid nitrogen using 25% (v/v) glycerol in the mother liquor as cryoprotectant. Diffraction data were collected at 100 K at SSRL beamline 12–2. Diffraction quality crystals of #4900-CR9114 Fab were obtained by mixing 0.5 μl of the concentrated protein (7.0 mg/ml) in 20 mM Tris, pH 8.0, 150 mM NaCl, and 0.02% NaN_3 with 0.5 μl of a reservoir solution containing 0.1 M sodium citrate pH 5.5 and 1.64 M ammonium sulfate at 22 ºC. The crystals were flash-cooled in liquid nitrogen using 50% saturated sodium malonate dibasic in the mother liquor as cryoprotectant. Diffraction data from the complex crystals were collected at 100K at SSRL beamline 12–2. HKL2000 (HKL Research, Inc.) was used to integrate and scale the data (table S1).

The structure of the complex between #4454 and CR9114 Fab was determined by molecular replacement (MR) using the program Phaser (57). The initial model for MR was the refined mini-HA #3964 (equivalent to #4157 but on A/California/04/2009 (ACP41105) background) structure from a #3964-CR9114 Fab complex (determined in our lab but not described here) and CR9114 Fab (PDB ID 4FQH). Two Fabs and two #4454 mini-HAs were found in the asymmetric unit. Initial rigid body refinement was performed using program Phenix (58). Further model rebuilding was performed using the graphics program Coot (59) and refined with Phenix. The structure was refined with data (99.9 % complete) to 4.30 Å. The resolution at which I/σ is ≥2 is 4.45 Å (99.9% complete). Final refinement statistics are summarized in table S1.
The structure of the complex between #4900 and CR9114 Fab was determined by molecular replacement (MR) using the program Phaser (57). The initial model for MR was the refined #3964 structure from the #3964-CR9114 Fab complex, the HA structure of A/California/04/2009 (H1N1) (PDB ID 4M4Y), and the CR9114 Fab structure (PDB ID 4FQH). One Fab and one #4900 mini-HA were present in the asymmetric unit. Initial rigid body refinement was performed using program Phenix (58). Further model rebuilding was performed using the graphics program Coot (59) and refined with Phenix. The structure was refined with data (99.9 % complete) to 3.60 Å. The resolution at which I/σ is ≥2 is 3.66 Å (100% complete). Refinement of antibody structures is almost always complicated due to flexibility in the hinge or 'elbow angle' between the variable and constant domains. This inherent flexibility allows the intact antibody to adjust its binding of the separate Fab arms in the intact IgG to the antigen, wherever possible, to achieve bivalent binding and increase avidity against microbial pathogens. In the final refined model of the CR99114 Fab complex with #4900, the mini-HA and V_H domain of the CR9114 Fab fit the electron density well, while the constant region of the CR9114 Fab is less ordered as reflected by higher B values for the antibody C_L (213 $Å^2$) and C_H1 (200 $Å^2$) domains compared to the average B values of mini-HA (140 $Å^2$) or antibody variable domains V_H (109 $Å^2$) and V_L (165 $Å^2$). The antibody- antigen interface is formed by the HA and only the V_H domain of the CR9114 Fab. This flexibility in the other antibody domains likely contributes to slightly higher Rcryst and Rfree values than if all antibody domains were well ordered and also to the 3.6 Å limit of the x-ray data. Final refinement statistics are summarized in table S1.

Immunization, influenza challenge and statistical analysis

All animal experiments were approved and performed in accordance with local legislation on animal experiments. Mice (BALB/c, female, 6–8 weeks old, n=10–14 per group) received intramuscular (i.m.) immunizations (three times unless specified otherwise) in hind legs with 30 μg mini-HAs adjuvanted with 10 μg Matrix-M (Novavax AB, Uppsala, Sweden) at 3-week intervals. A group of mock-immunized mice (buffer only) was included as negative control. Four weeks after the last immunization and prior to challenge, a pre-challenge mouse blood sample was obtained via retro-orbital cannulation or submandibular bleeding.

For serum transfer studies, groups of donor mice (n=60) were immunized with mini-HA constructs or mock immunized with vehicle according to the regimen described above. Four week after the final immunization, serum was isolated, pooled and transferred (400 μl, intraperitoneally) to naïve recipient mice at three consecutive days

prior to challenge. The absence and presence of FL HA-specific antibodies in recipient mice prior and after transfer of serum was confirmed by ELISA.

As an established positive control for the challenge experiments, bnAb CR6261 was administered at 15 mg/kg intravenously (i.v.) one day before the challenge. Mice were challenged intranasally (i.n.) with 12.5 or 25 LD50 of influenza virus under ketamine/xylazine anesthesia. After challenge, mice were monitored for survival, bodyweight loss and clinical score for up to 21 days.

To evaluate immunogenicity and protective efficacy in cynomolgus macaques, a cohort of male cynomolgus macaques (median age 4 years, range 4.5-12.1 years, median weight 7.8 kg, range 5.1-11.0 kg) pre-screened negative for serum antibodies against alpha herpes virus, STLV, SRV,flu A NP and HAI against the challenge virus, were used. Animals were randomly allocated to 3 groups of 6 animals each, using a randomized block design taking age and weight into account. Data-loggers measuring body temperature with 15 min interval were implanted abdominally, followed by a 1 month recovery period after which the immunization regimen started. One group received 2 intramuscular (i.m.) immunizations with the human dose (0.5 mL) of Inflexal® V season 2013 (Crucell, Bern, Switzerland) containing 15 µg FL HA of each A/California/7/2009 (H1N1), A/Texas/50/2012 (H3N2) and B/Massachusetts/2/2012, in agreement with official guideline immunization regimen for naïve persons as advocated by healthcare agencies (CDC, RIVM). The second group received 3 i.m. immunizations with 150 µg mini-HA #4900 protein adjuvanted with 50 µg Matrix-M in a volume of 0.5 mL. The third group was a negative control group receiving 3 times 0.5 mL PBS i.m. The immunizations were performed with a 4-weeks interval. Four weeks after the final immunizations animals were challenged intrabroncheally with $4x10^6$ $TCID_{50}$ H1N1 A/Mexico/InDRE4487/2009, which is the dose that was established during setup of the model based on Safronetz et al. (60). During the 21 day follow-up period, clinical signs were recorded daily. Animals were anesthetized on day 1, 2, 4, 6, 8, 10, 14 and 21 during which bodyweight was measured, tracheal swabs taken to determine viral load by real-time PCR (61), and serum samples taken. At the end of the study, data-loggers were removed and body temperature data analyzed, except for 1 animal in the mini-HA #4900 treatment group for which no data were recorded due to data-logger failure. A reference 24-hour body temperature cycle was reconstructed per animal using a 21-day window prior to start of the immunizations. The net increase in body temperature during the 21 day post-challenge follow-up period was calculated as difference relative to the upper 95% confidence limit of the reference cycle at corresponding clock times. The lower limit of the temperature difference was set at zero to reduce the impact of lower body temperatures during post-challenge anesthesia. The AUC of the net temperature increase was subsequently calculated over intervals of day 0-3, day 0-8 and day 0-21. One animal in the Inflexal treatment group died at the end of day 8 of viral pneumonia and was excluded from the day 0-21 interval analysis. Consistent with observations during setup of the model in a previous study, no major differences in clinical signs and body weight before and after challenge were observed, and residual differences were attributed to repeated anesthesia and therefore not further analyzed.

FL HA ELISA

To measure mini-HA–induced antibody responses against selected FL HA, Maxisorp 96-well plates (Nunc™, Thermo Scientific, Bremen, Germany) were coated with 0.5 µg/ml recombinant FL HA (Protein Sciences, Meriden, CT) O/N at 4 °C. Plates were washed with PBS (Gibco®, Life Technologies™, Paisley, UK) containing 0.05% Tween-20 (Calbiochem®, Merck Millipore, Darmstadt, Germany) (PBS-T) and subsequently blocked with block buffer (PBS containing 2% dried skimmed milk (Difco™, BD, Breda, the Netherlands) for 1 hour at RT. After washing, serum was added to the plate in duplicate, serially diluted in block buffer and incubated for 1 hour at RT. Following a wash with PBS-T, a 1:2000 dilution of Goat-anti-Mouse IgG-HRP (KPL, Gaithersburg, MD, USA) was added to the plate for mouse samples, or a 1:5000 dilution of Goat-anti-Monkey IgG HRP (Bio-Rad, Hercules California, USA) for macaque samples. After incubation for 1 hour at RT, plates were washed and developed using OPD substrate (Thermo Scientific). The colorimetric reaction was stopped after 10 min by adding 1M H_2SO_4. The optical density (OD) was measured at 492 nm. The OD of each sample dilution was then quantified against the standard curve included on each plate, consisting of a murine IgG2a version of CR9114 for mouse samples or CR9114 for macaque samples, and the final concentration per sample calculated by a weighted average, using the squared slope of the standard curve at the location of each quantification as weight. Negative samples were set at the limit of detection (LOD), defined as the lowest sample dilution multiplied by the lowest standard concentration, with an OD response above the lower asymptote of the standard curve and background. ELISA titers were expressed as log10 ELISA Units (EU) per ml.

CR9114 competition ELISA

Plates were coated with purified polyclonal rabbit anti His-Tag IgG (GenScript USA Inc., NJ, USA) O/N at 4 °C followed by washing. After blocking with 2% BSA in PBS for 1 hour at RT and washing, plates were incubated with a titrated amount of His-tagged FL HA for 2 hours at RT. Plates were washed and serum added to the plate in duplicate, serially diluted in block buffer, and incubated for 1 hour at RT, followed by addition of a titrated amount of biotinylated human IgG1 CR9114 and incubation for another hour at RT. After washing, streptavidin-HRP was added and incubated for 1 hour at RT, followed by washing and OPD development. The percentage competition was calculated as follows: % competition = (A-P)/Ax100), where A is the maximum OD signal of CR9114 binding to FL HA when no serum is present, and P is the OD signal of CR9114 binding to FL HA in presence of serum at a given dilution (26). Positive and negative controls consisted of competition with monoclonal antibodies CR9114 and CR8020 (3, 5) and showed 100% and 0% competition, respectively (data not shown).

Hemagglutination inhibition assay

Non-specific agglutination inhibitors were removed from serum samples by overnight incubation at 37 °C with *Vibrio cholerae* neuraminidase (Sigma-Aldrich, St. Louis, Missouri, USA), which was subsequently inactivated by incubation with 2.5% sodium citrate for 30 minutes at 56 °C. PBS (Gibco, Life Technologies; Carlsbad, California,

USA, pH 7.4) and 0.5% turkey red blood cells (bioTRADING Benelux B.V., Mijdrecht, the Netherlands) were added, samples were incubated for 2 hour at 4 °C and subsequently spun down. Twofold serial dilutions of the supernatant in PBS were prepared in duplicate, mixed by agitation with 4 HA units of H1N1 A/California/07/2009 (wild-type) virus and incubated for 1 hour at room temperature, followed by addition of 1% Turkey red blood cells incubation for another hour at room temperature, and the hemagglutination status of each well determined. The assay titer of a given serum sample was defined as the reciprocal of the highest dilution where no hemagglutination inhibition was observed.

Virus neutralization assay

Madin–Darby Canine Kidney (MDCK) cells were seeded in Immulon 2HB (Thermo Scientific, Bremen, Germany) 96-well plates, at 15,000 cells per well in assay medium (Dulbecco's Modified Eagle Medium [DMEM]) containing L-glutamine, 3 μg/mL trypsin/EDTA, and 1% (w/v) penicillin/streptomycin stock solution all from Gibco, Invitrogen Ltd (Life Technologies, Paisley, UK) and allowed to attach for a minimum of 3 hours. Duplicate serial dilutions of heat inactivated (30 min at 56 °C) serum samples were prepared in assay medium without trypsin/EDTA and mixed with H5N1 reassortant A/Hong Kong/156/97 (rgPR8-H5N1 6:2 reassortant, containing HA and NA from H5N1 A/Hong Kong/156/97) virus in assay medium containing trypsin/EDTA, for 1 hour at 37 °C, 10% CO_2. Virus and serum were subsequently added to the MDCK cells at a final concentration of 100 $TCID_{50}$ virus per well and incubated for 20 hours at 37 °C, 10% CO_2. Cells were fixed with 80% acetone for 10 minutes and air-dried, plates washed with PBS containing 0.05% Tween-20 (Calbiochem®, Merck Millipore, Darmstadt, Germany) (PBS-T) and labeled with biotin conjugated mouse anti-influenza A nucleoprotein (H16-L10-4R5, produced in house) for 1 hour. After washing with PBS-T, plates were incubated with Streptavidin-HRP (BD Biosciences, Breda, the Netherlands) for 1 hour, washed with PBS-T and ABTS substrate (Roche, Basel, Switzerland) added. Absorbance was read at 405 nm using a BioTek®reader (PerkinElmer, Groningen, the Netherlands) after 45 min.

Pseudoparticle neutralization assay

Pseudoparticles expressing FL HA were generated as previously described (62). Neutralizing antibodies were determined using a single transduction round of HEK293 cells with H5 HA A/Vietnam/1194/04 pseudoparticles encoding luciferase reporter gene, as described previously (34), with a few modifications. Briefly, heat-inactivated (30 minutes at 56 °C) pre-challenge serum samples were 3-fold serially diluted in growth medium (MEM Eagle with EBSS [Lonza, Basel, Switzerland] supplemented with 2 mM L-Glutamine [Lonza], 1% Non-Essential Amino Acid Solution [Lonza], 100 U/ml Pen/Strep [Lonza] and 10% FBS [Euroclone, Pero, Italy]) in triplicate in 96-well flat bottom culture plates and a titrated number of H5 A/Vietnam/1194/04 pseudoparticles (yielding 106 relative luminescence units [RLU] post-infection) was added. After 1 hour of incubation at 37 °C, 5% CO_2, 10^4 HEK293 cells were added per well. After 48 hours of incubation at 37 °C, 5% CO_2, luciferase substrate (Britelite Plus, Perkin Elmer,

Waltham, MA) was added and luminescence was measured using a luminometer (Mithras LB 940, Berthold Technologies, Germany) according to the manufacturers' instructions.

Antibody-dependent cellular cytotoxicity (ADCC) surrogate assay

Human lung carcinoma–derived A549 epithelial cells (ATCC CCL-185) were maintained in Dulbecco's Modified Eagle Medium (DMEM) supplemented with 10% heat inactivated fetal calf serum at 37 °C, 10% CO_2. Two days before the experiment, A549 cells were transfected with plasmid DNA encoding FL HA proteins as indicated in the figure legends, using Lipofectamine 2000 (Invitrogen) in Opti-MEM (Invitrogen). One day before the assay, transfected cells were harvested and seeded in white 96-well plates (Costar). After 24 hours, samples were diluted in assay buffer (4% ultra-low IgG FBS [Gibco] in RPMI 1640 [Gibco]) and heat inactivated for 30 min at 56 °C, followed by serial dilution in assay buffer. The cells were replenished with fresh assay buffer and ADCC Bioassay effector cells (a stable Jurkat cell line expressing mouse FcγRIV for mouse samples or human FcγRIIIa (V158 variant) for macaque samples), human CD3γ, and an NFAT- response element driving expression of a luciferase reporter gene (35) were added and incubated for 6 hours at 37 °C at a target-effector ratio of 1 to 4.5. Cells were equilibrated to room temperature for 15 min before Bio-Glo Luciferase Assay System substrate (Promega) was added. Luminescence was read out after 10 min on a Synergy Neo microplate reader (Biotek). Data are expressed as fold induction of signal in the absence of serum.

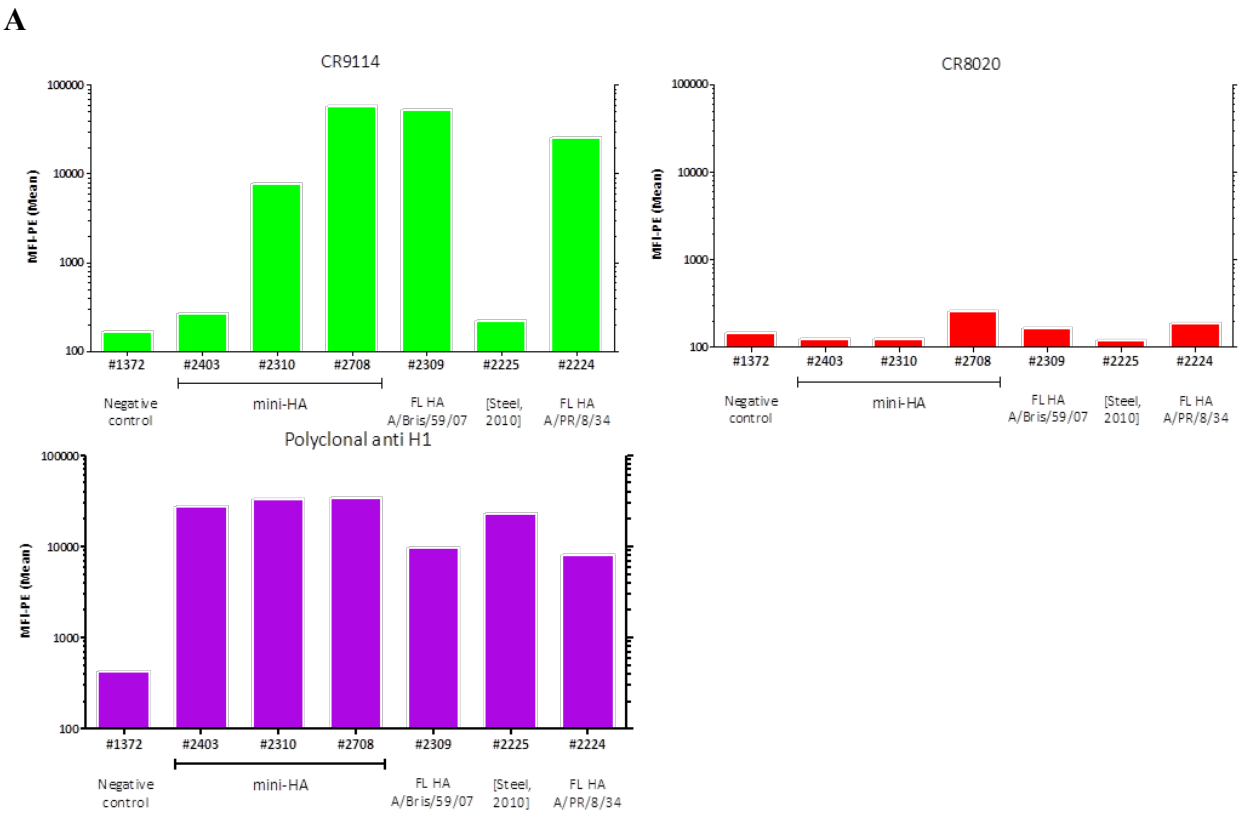
A
CR9114
CR8020
Polyclonal anti H1
MFI-PE (Mean)
100000
10000
1000
100
#1372
#2403
#2310
#2708
#2309
#2225
#2224
Negative control
mini-HA
FL HA A/Bris/59/07
[Steel, 2010]
FL HA A/PR/8/34

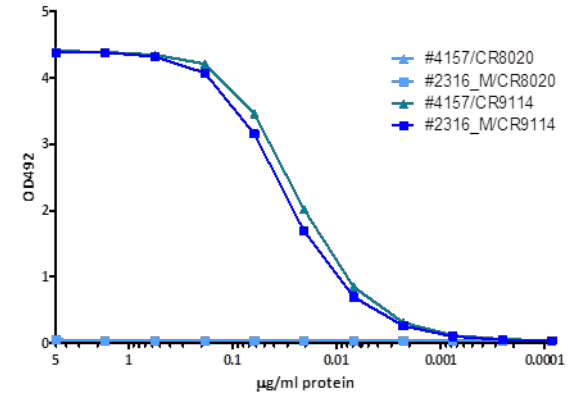
B
#4157/CR8020
#2316_M/CR8020
#4157/CR9114
#2316_M/CR9114
OD492
µg/ml protein

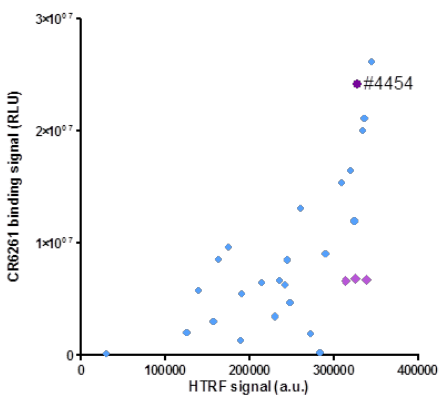
C
#4454
CR6261 binding signal (RLU)
HTRF signal (a.u.)

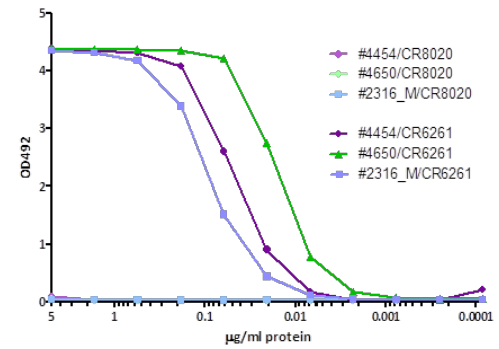
D
#4454/CR8020
#4650/CR8020
#2316_M/CR8020
#4454/CR6261
#4650/CR6261
#2316_M/CR6261
OD492
µg/ml protein

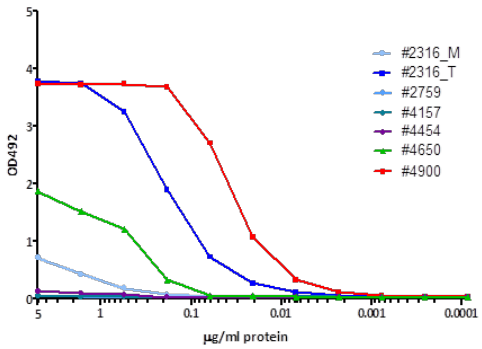
E
#2316_M
#2316_T
#2759
#4157
#4454
#4650
#4900
OD492
µg/ml protein

F

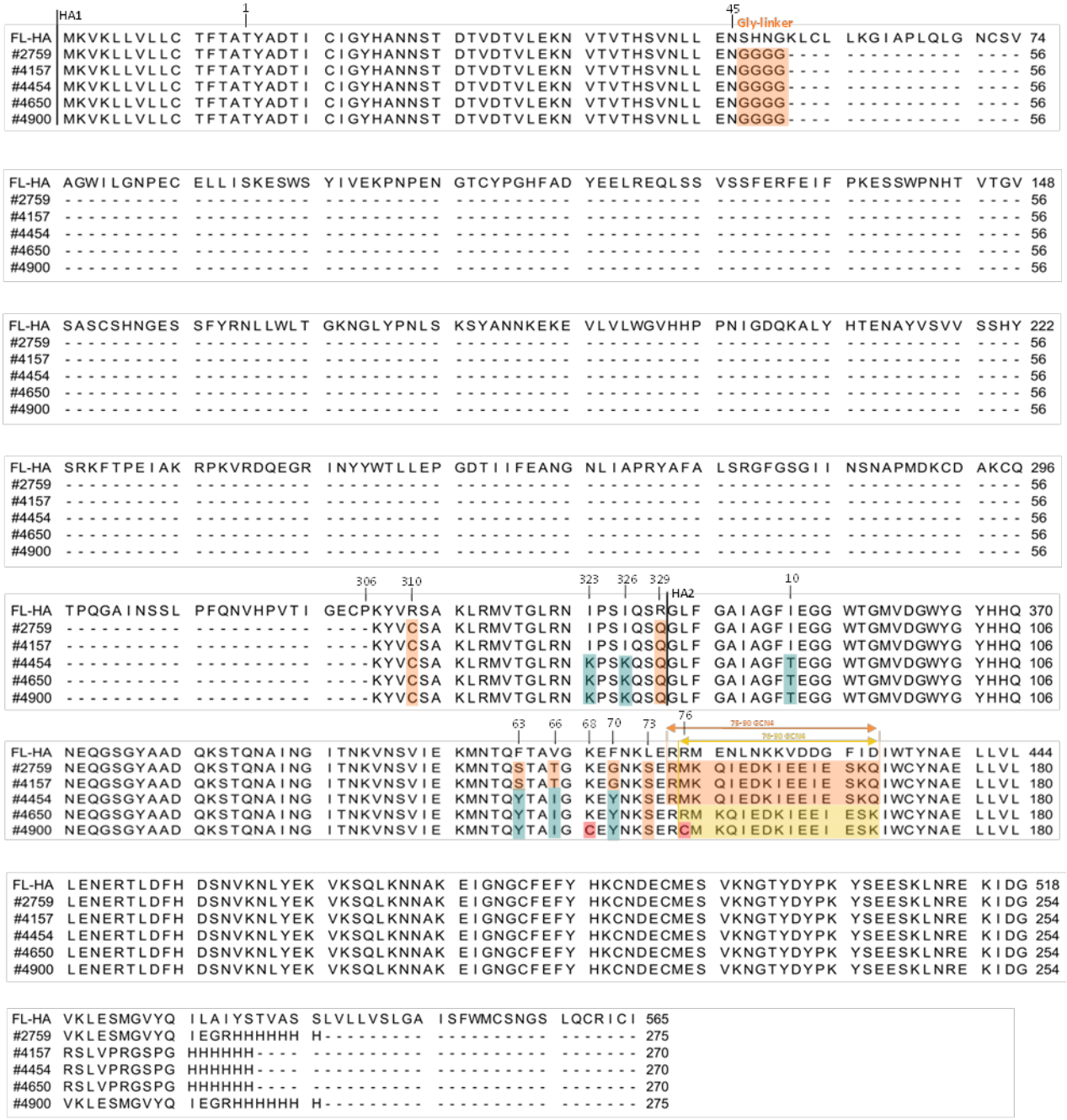

Fig. S1. Representative results for mini-HA design. (**A**) Binding of CR9114 to membrane-bound mini-HA variants. HEK293F cells transfected with constructs encoding surface-expressed mini-HA variants or FL HA positive controls were analyzed by FACS. As a negative control, cells were transfected with construct #1372 encoding the influenza M2 protein. The upper left panel shows the improvement of CR9114 binding as mini-HAs evolve. No or very low binding is observed for a previously published construct (48)

(#2225), which is based on HA from A/Puerto Rico/8/34. H3 specific antibody CR8020 was used as negative control (right panel). Staining with polyclonal anti-H1 antibodies was used to verify protein expression (lower panel). (**B**) Binding of CR9114 to the best soluble mini-HA from stage II (#4157) and monomeric FL HA A/Brisbane/59/07 (#2316_M) in His-tag ELISA. CR8020 was used as negative control. (**C**) Testing mini-HA library candidates in mammalian cells. Selected yeast library clones were expressed in HEK293F cells. The CR6261 binding and protein expression (HTFR) signals are depicted. The parental mini-HA #4157 is indicated in light purple diamonds and mini-HA #4454 in a dark purple circle. (**D**) Binding of CR6261 to mini-HA #4650, its library parent #4454 and monomeric FL HA (#2316_M). CR8020 was used as negative control. (**E**) CR9114 binding to mini-HAs and FL HA (monomeric #2316_M and trimeric #2316_T) in a CR9114 sandwich (multimer) ELISA. (**F**) Alignment of FL HA A/Brisbane/59/2007 with the lead candidates #4157 (stage II), #4454 (stage III), #4650 (stage IV) and #4900 (stage V). The residue numbering used to indicate the mutated residues is positioned on the top of the alignment and refers to the H3 numbering of HA1 and HA2 subunits. The color code is the same as in Fig. 1: orange for mutations generated in stage I and II, teal for stage III, yellow for stage IV and red for stage V.

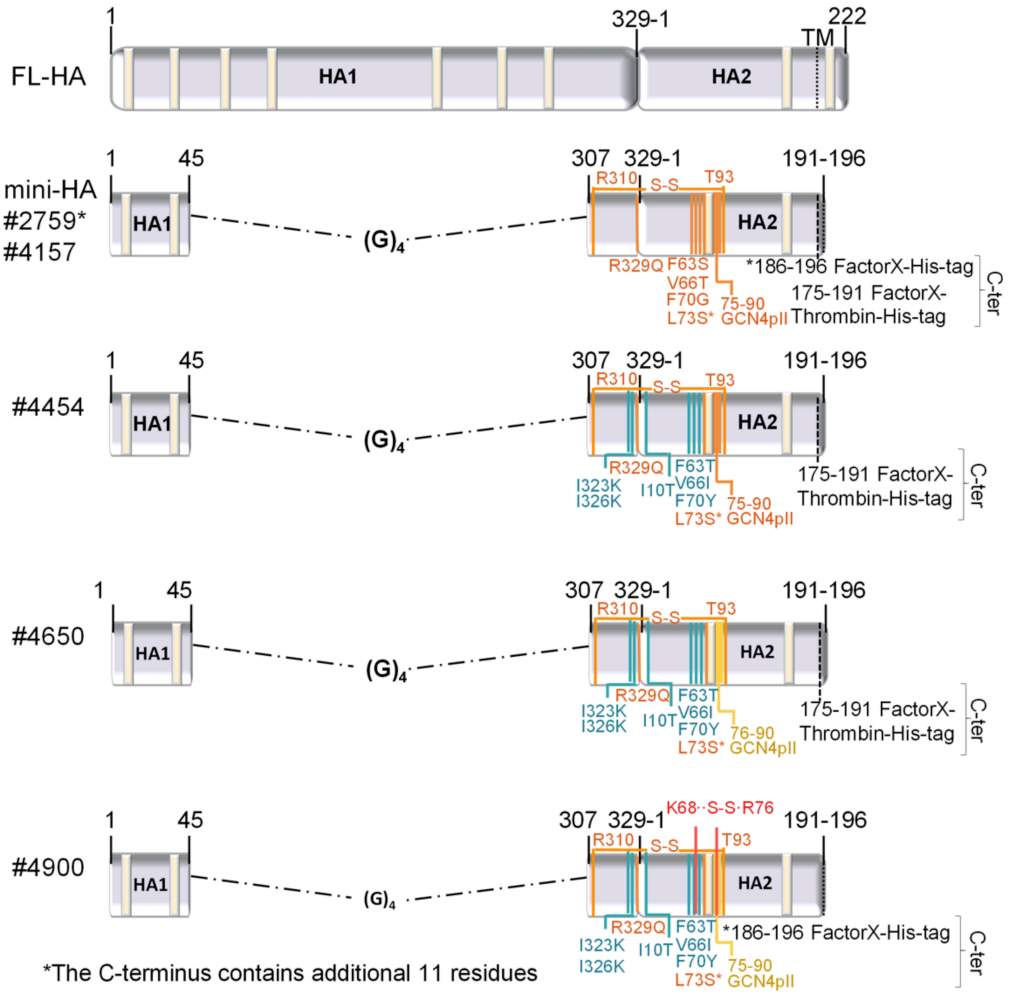

Fig. S2. Overall architecture of the designed mini-HA constructs. Parental FL HA (A/Brisbane/59/07) is compared to selected mini-HA construct designs with specific modifications depicted and color coded as in Fig. 1, A and B. Whitish cream thicker stripes indicate putative N-glycosylation sites.

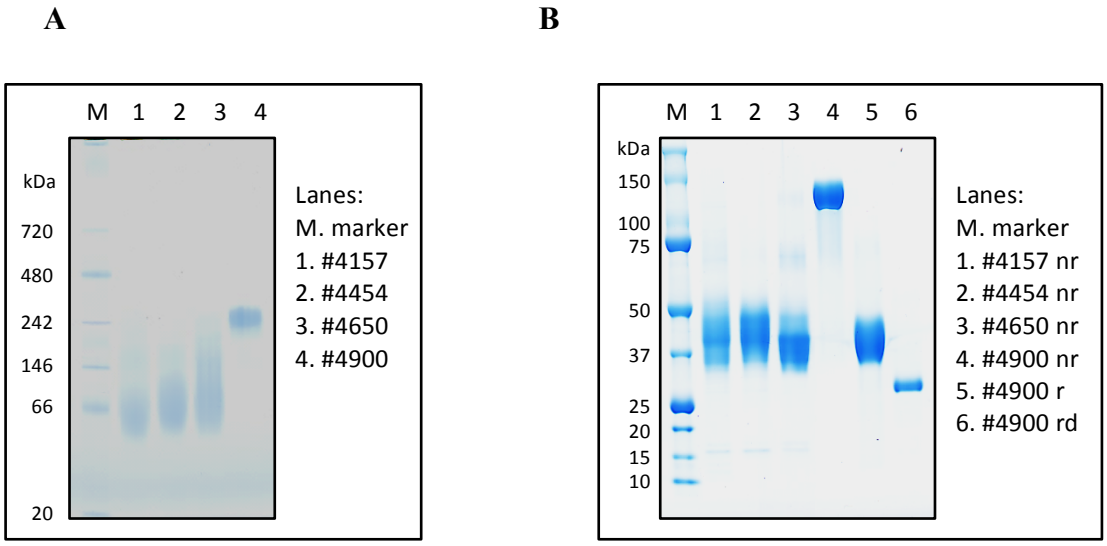

Fig. S3. Characterization of purified mini-HA candidates. (**A**) Native PAGE. (**B**) SDS PAGE under non-reducing (nr) and reducing (r) condition, and upon sample deglycosylation (d).

A

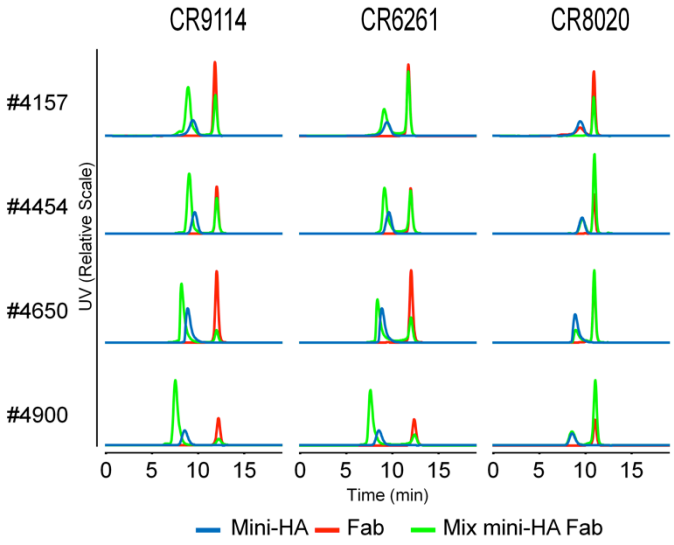

B

CR9114

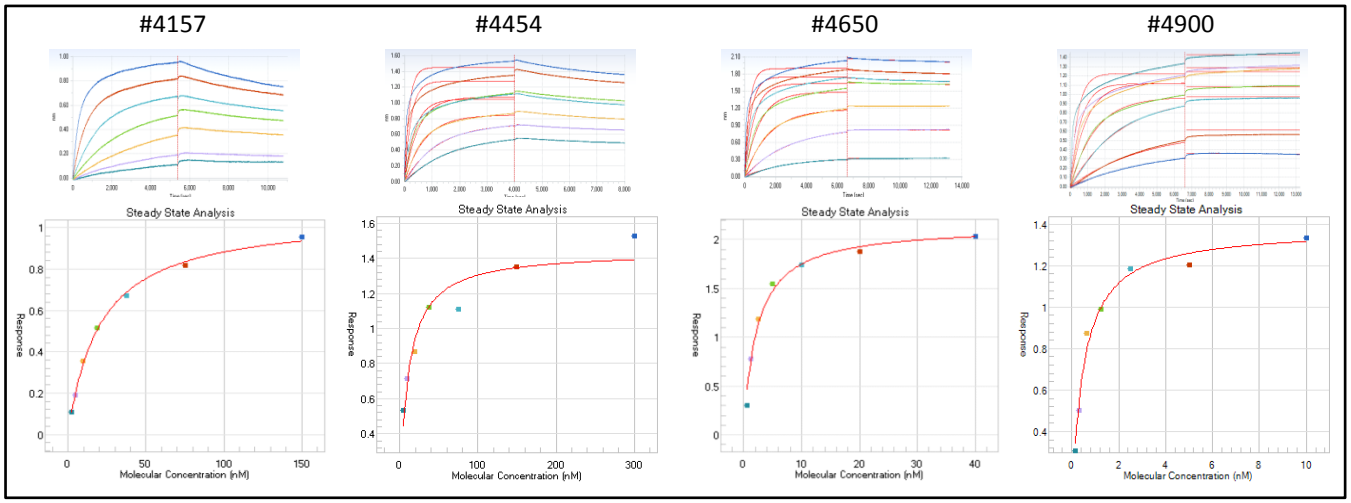

CR6261

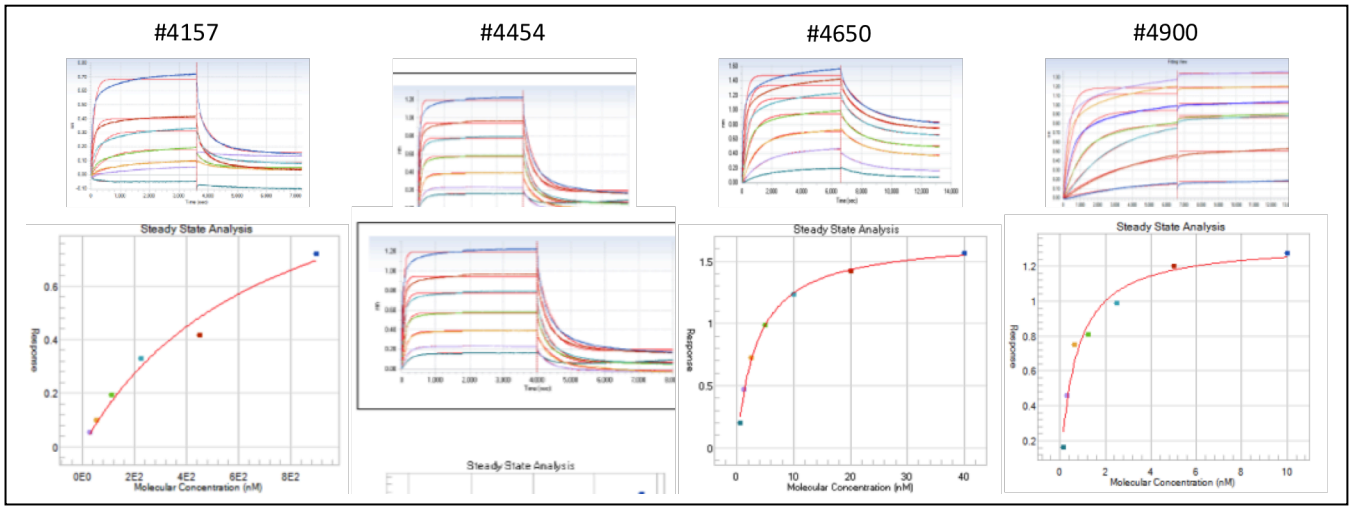

Fig. S4. Binding of bnAbs to selected mini-HA candidates. (A) Binding of Fabs of bnAbs CR9114 and CR6261 to mini-HAs in solution analyzed by Size Exclusion Chromatography (SEC). The peak shift of the mini-HA in presence of bnAbs to a shorter retention time is indicative of complex formation. No binding to mini-HA is observed for group 2 specific CR8020 Fab. (B) Binding of mini-HA candidates to CR9114 (top panel) and CR6261 (bottom panel) using biolayer interferometry. The individual real-time binding curves for immobilized monoclonal antibodies exposed to varying concentrations of mini-HA and the steady state analysis (assuming a 1:1 binding model) were used for the K_D estimation. Different scales are used for different samples.

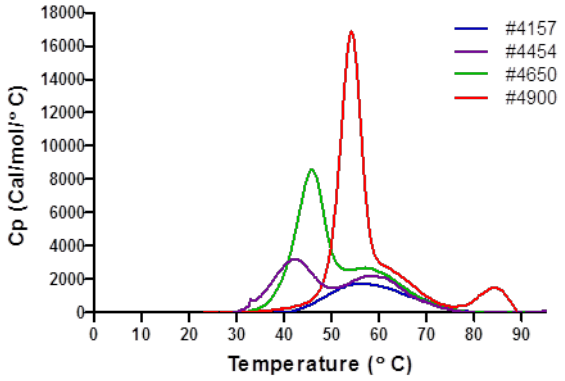

Fig. S5. Differential scanning calorimetry: analysis of the thermal unfolding profiles of selected mini-HAs. Excess heat capacity curves are shown for samples containing 18 μM mini-HA in PBS. The temperature scans were performed between 20 and 90 °C at a scan rate of 1 °C/min and were corrected by subtracting the sham thermal profiles of PBS. All constructs showed a common thermal transition with a mid-point transition temperature (T_m) of ~59 °C, which may be attributed to unfolding of the mini-HA monomer unit. In addition, all mini-HAs, except #4157, displayed an earlier transition, with the T_m increasing from 42 to 54 °C during the design process that may correspond to dissociation of the dimeric and trimeric interfaces of the mini HA constructs, respectively. Furthermore, mini-HA #4900 exhibits another small transition above 80 °C, which is possibly attributable to the cooperative dissociation of the GCN4 helical segments as previously reported (63, 64). The thermal unfolding patterns of the mini-HAs clearly illustrates that the stability of the mini-HAs evolved during the design.

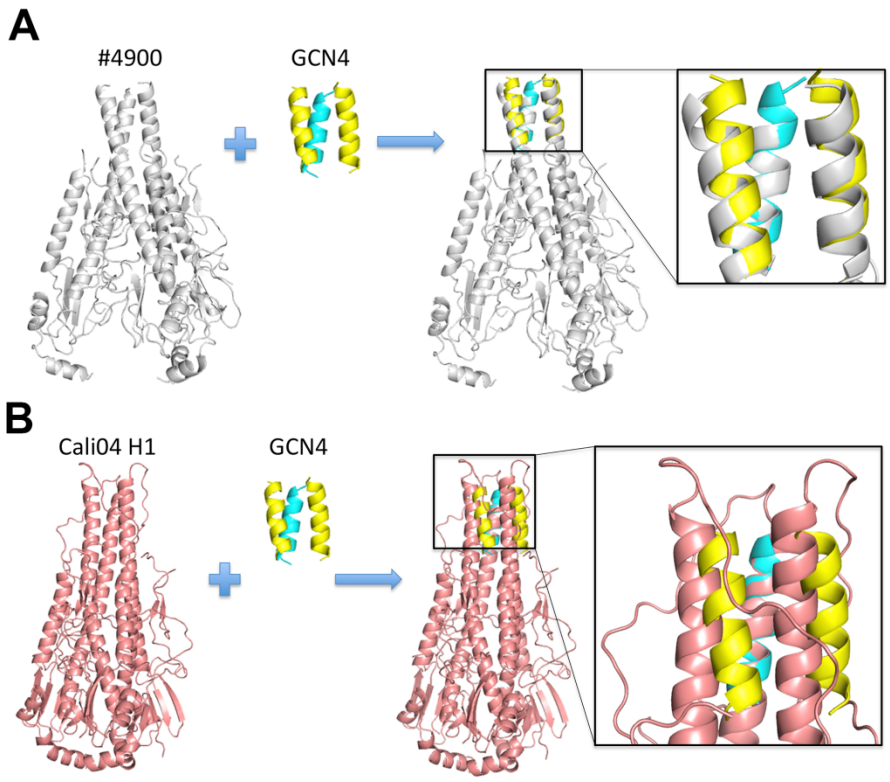

Fig. S6. **Superimposition of mini-HA #4900 with the GCN4 structure (PDB ID 1CZQ) and HA from A/California/04/2009 (H1N1) (Cali04 HA, PDB ID 4M4Y)**. (**A**) Superimposition of #4900 (in grey) with the GCN4 structure (in yellow and cyan). Standard view of #4900 (in grey) and GCN4 (in yellow and cyan). The helix of GCN4 was used to superimpose the corresponding region on #4900. The overall structure of the helices of the GCN4 motif in #4900 superimpose well with the GCN4 structure. (**B**) Superimposition of the equivalent mini-HA region from the Cali04 HA structure (in orange) with GCN4 (in yellow and cyan). The cyan helix of GCN4 was used to superimpose with the corresponding residues of Cali04 mini-HA. The overall structure and relative configuration of the corresponding N-terminal end of the long CD helix around the trimer axis of Cali04 H1 HA is significantly different compared to the GCN4 structure.

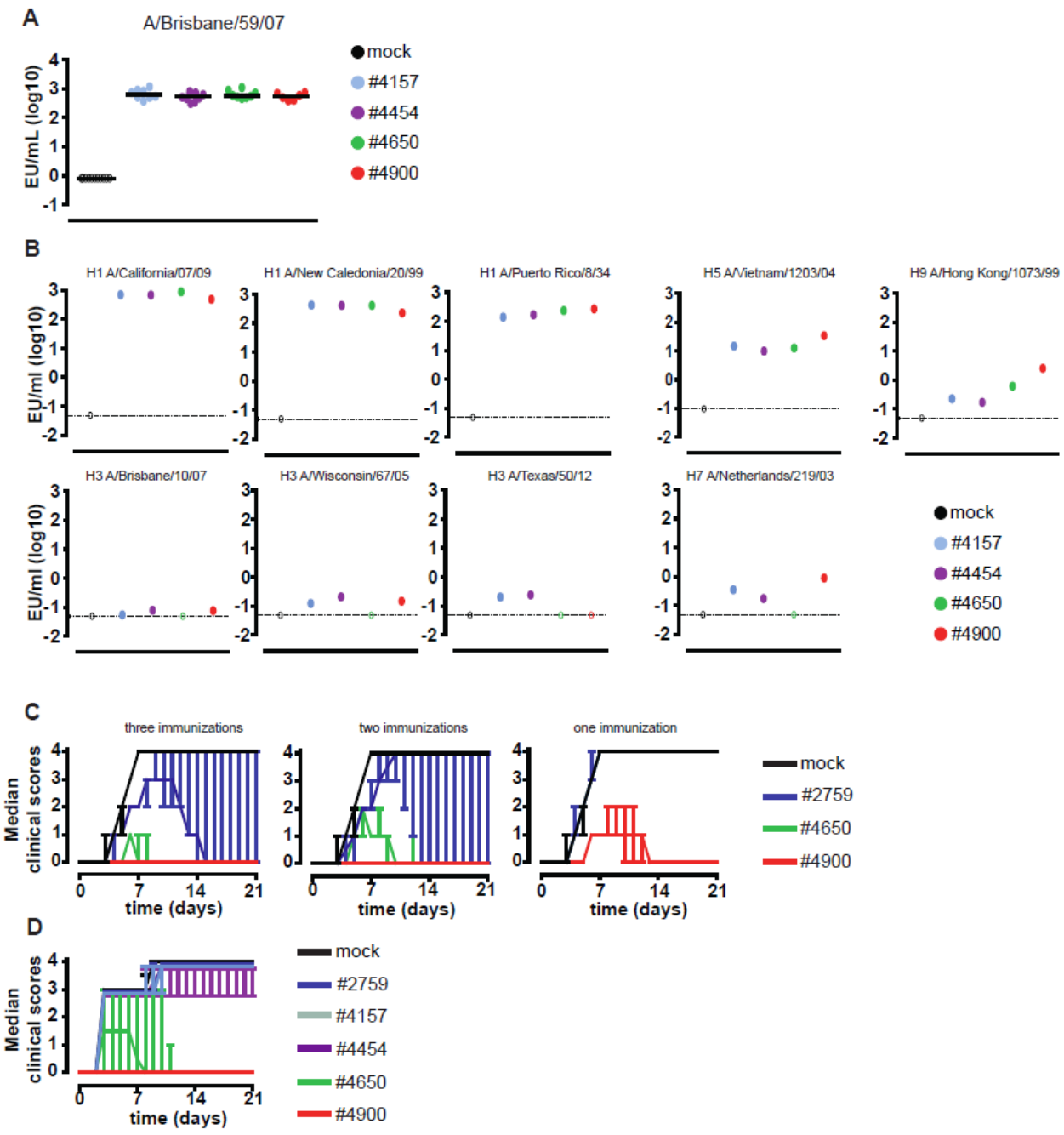
A
A/Brisbane/59/07
EU/mL (log10)
mock
#4157
#4454
#4650
#4900
B
H1 A/California/07/09
H1 A/New Caledonia/20/99
H1 A/Puerto Rico/8/34
H5 A/Vietnam/1203/04
H9 A/Hong Kong/1073/99
H3 A/Brisbane/10/07
H3 A/Wisconsin/67/05
H3 A/Texas/50/12
H7 A/Netherlands/219/03
EU/ml (log10)
mock
#4157
#4454
#4650
#4900
C
three immunizations
two immunizations
one immunization
Median clinical scores
time (days)
mock
#2759
#4650
#4900
D
Median clinical scores
time (days)
mock
#2759
#4157
#4454
#4650
#4900

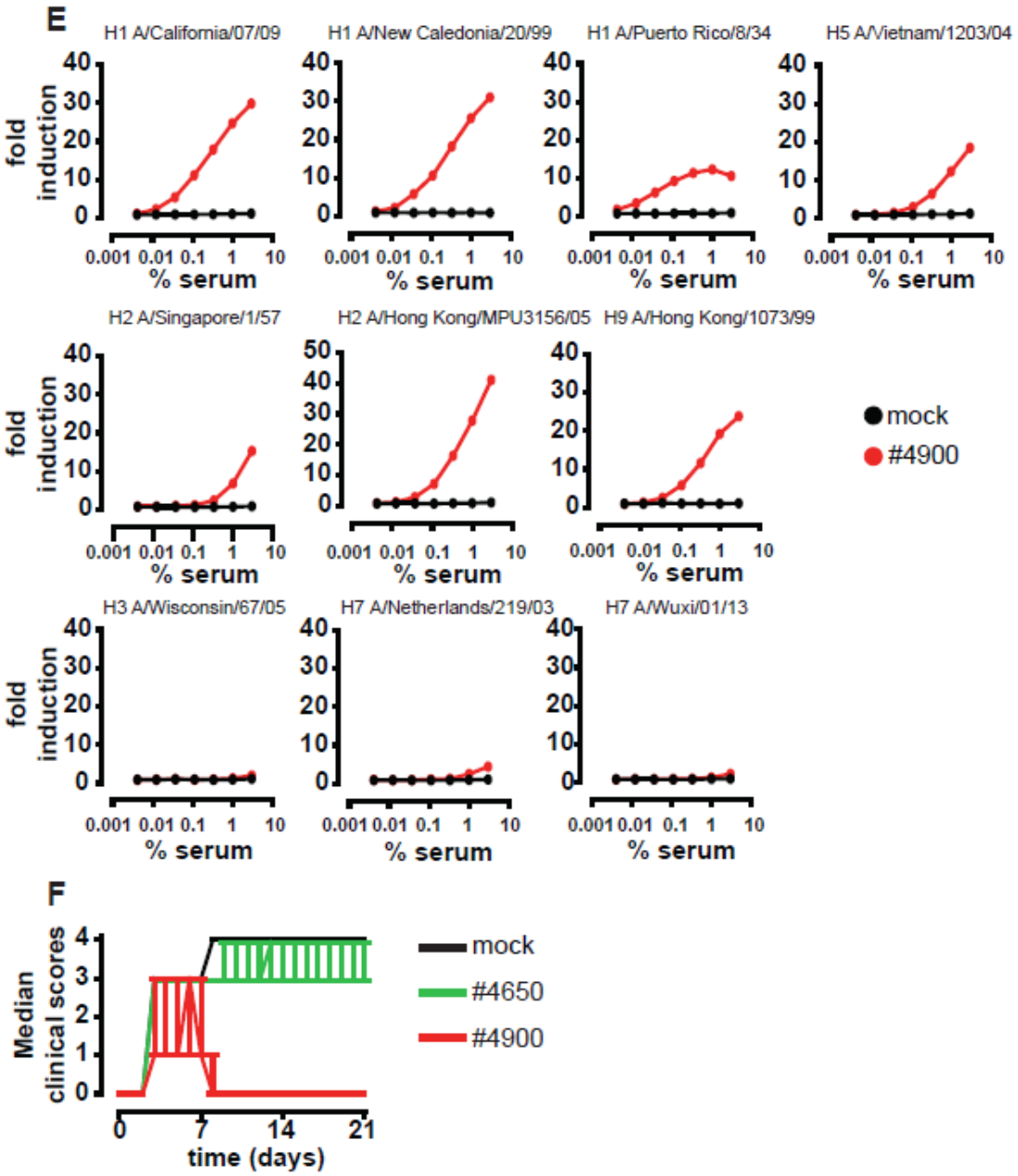

Fig. S7. Immunogenicity and protective ability of mini-HAs in mice (**A**) Binding of pre-challenge mini-HA-specific antibodies to FL HA from H1N1 A/Brisbane/59/07. Each dot represents results obtained with serum from individual mice (6–11 per group). Open symbols indicate samples that were below limit of detection using a serum start dilution of 1/800. Bars represent medians. (**B**) Binding of pre-challenge mini-HA-specific antibodies to FL HA from group 1 and 2 influenza A strains. Each dot represents result obtained with the serum from 10-60 mice from different studies and pooled per mini-HA immunization group. Open symbols indicate samples that were below limit of detection using a serum start dilution of 1/50. Line represents limit of detection. (**C**) Median clinical score on mini-HA and mock-immunized mice challenged with H1N1 A/Puerto

Rico/8/34. (**D**) Median clinical score on mini-HA and mock-immunized mice challenged with H5N1 A/Hong Kong/156/97. (**E**) Breadth of ADCC. ADCC surrogate assays with A549 cells transfected with indicated FL HA and serum (pooled per immunization group) from additional experiments, using serum from mice immunized with #4900 mini-HA or mock-immunized. Data shown are the geometric mean of two replicates per measurement. (**F**) Median clinical score after passive immunization with sera from mice immunized with mini-HA or mock-immunized followed by challenge with H5N1 A/Hong Kong/156/97. Error bars denote interquartile range for all median clinical score data.

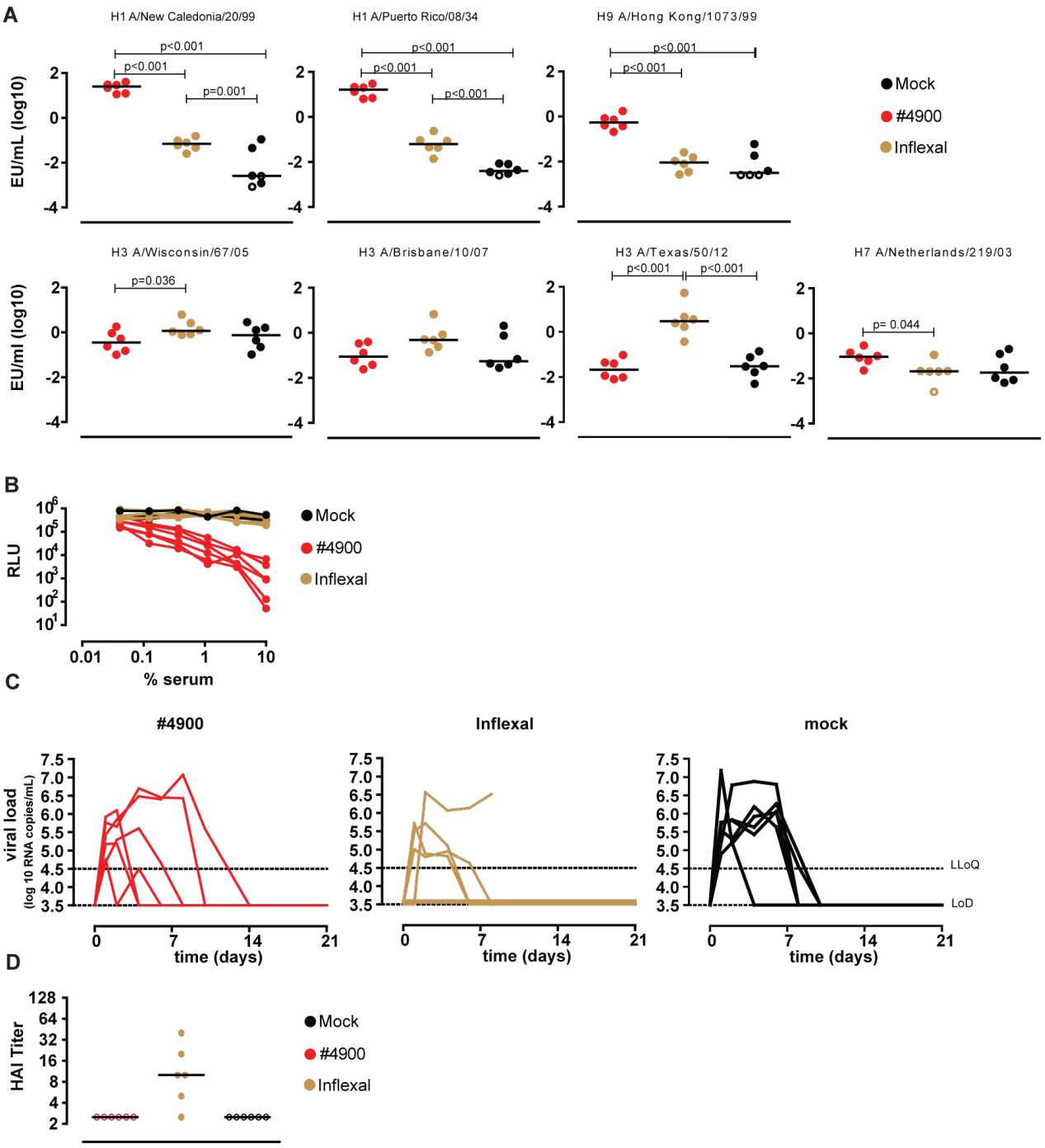
A
H1 A/New Caledonia/20/99
H1 A/Puerto Rico/08/34
H9 A/Hong Kong/1073/99
H3 A/Wisconsin/67/05
H3 A/Brisbane/10/07
H3 A/Texas/50/12
H7 A/Netherlands/219/03
EU/mL (log10)
EU/ml (log10)
p<0.001
p=0.001
p=0.036
p= 0.044
Mock
#4900
Inflexal
B
RLU
% serum
C
#4900
Inflexal
mock
viral load
(log 10 RNA copies/mL)
time (days)
LLoQ
LoD
D
HAI Titer

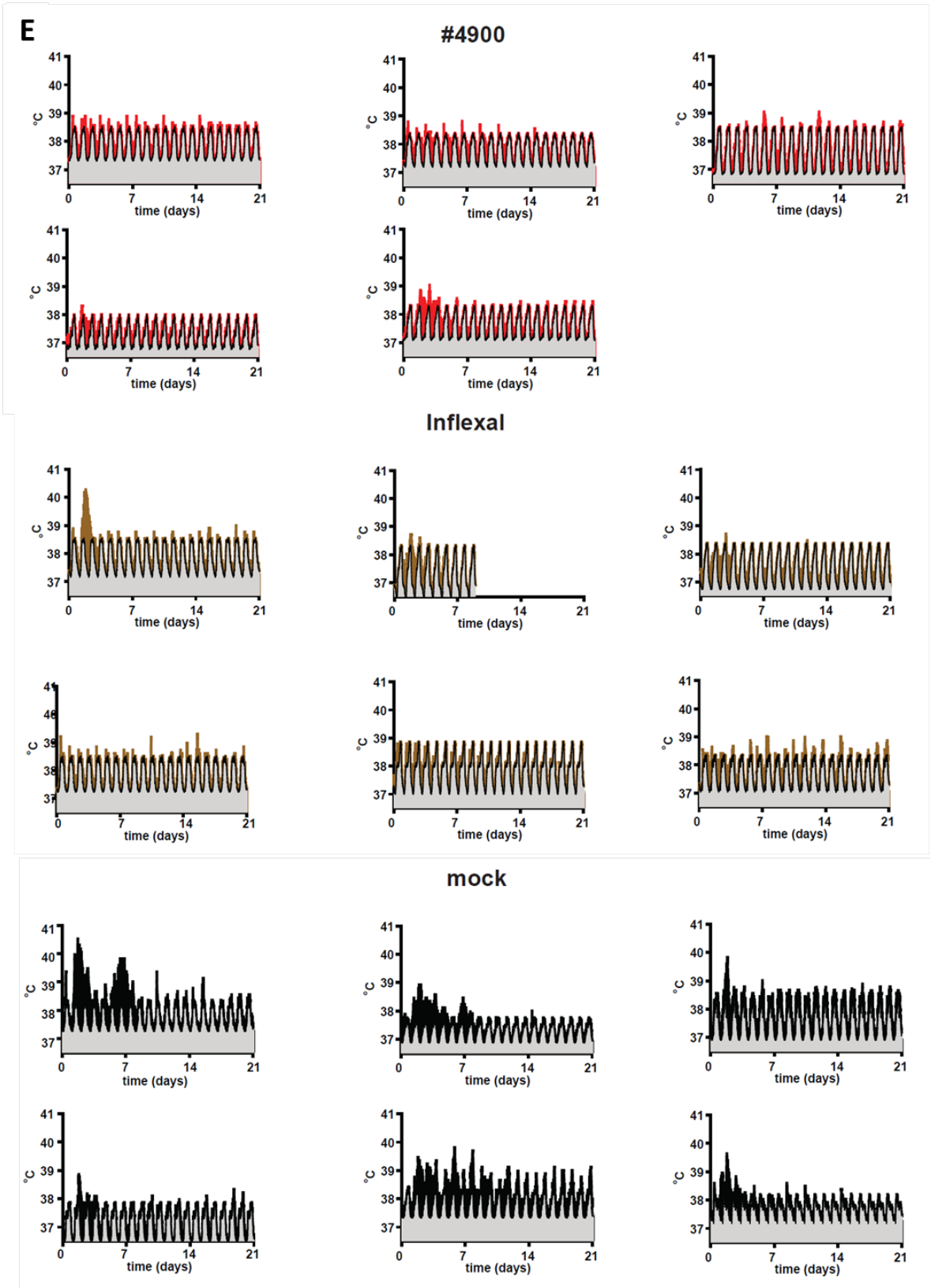
E
#4900
Inflexal
mock
°C
time (days)
0
7
14
21
37
38
39
40
41

Fig. S8. Immunogenicity and protective efficacy of mini-HA #4900 in cynomolgus macaques. (**A**) Binding of pre-challenge serum antibodies to FL HA from group 1 and 2 influenza A strains. Each dot represents an individual animal. Open symbols indicate samples that were below limit of detection using a serum start dilution of 1/50. Bars represent medians. (**B**) Neutralization of H5 HA A/Vietnam/1194/04 pseudovirus, with pre-challenge serum of individual animals. Data shown are the geometric mean of three replicates per measurement. (**C**) Tracheal influenza viral load post-challenge. Lower limit of quantification (LLoQ) and limit of detection (LoD) are indicated by horizontal dashed lines. (**D**) Pre-challenge HAI titers of individual animals against H1N1 A/California/07/09. Open symbols indicate samples that were below limit of detection using a serum start dilution of 1/10. (**E**) Body temperatures of individual animals post-challenge. Grey curves represent a reference 24-hour body temperature cycle, reconstructed using a 21-day window prior to start of the immunizations. For one animal in the H1 mini-HA treatment group, no data were recorded due to data logger failure. One animal in the Inflexal treatment group was analyzed up to point of death (day 8).

Table S1. Data collection and refinement statistics for #4454-CR9114 Fab and #4900-CR9114 Fab.

Data set	#4454/CR9114 Fab	#4900/CR9114 Fab
Space group	$P3_221$	R32
Unit cell (Å)	$a = b = 110.8$,	$a = b = 157.7$,
	$c = 359.2$	$c = 202.6$,
Resolution (Å) [a]	50.0-4.30	50.0-3.60
	(4.54-4.45, 4.45-4.37, 4.37-4.30)	(3.73-3.66, 3.66-3.60)
X-ray source	SSRL 12-2	SSRL 12-2
Unique reflections	18,316	11,619
Redundancy [a]	8.1 (6.8, 6.3, 6.0)	8.5 (8.4, 8.5)
Average I/σ(I) [a]	9.1 (2.0, 1.8, 1.2)	22.0 (2.0, 1.6)
Completeness [a]	99.9 (99.9, 99.4, 99.9)	99.9 (100.0, 100.0)
R_{sym} [a,b]	0.21 (0.69, 0.70, 0.92)	0.10 (0.83, 0.96)
R_{pim} [a,b]	0.08 (0.28, 0.29, 0.39)	0.04 (0.30, 0.35)
Mini-HAs in a.u.	2	1
Reflections in refinement	18,248	11,557
Refined residues	1,258	634
R_{cryst} [c]	0.26	0.35
R_{free} [d]	0.30	0.37
Refined B-values (Å^2)	180	158
Wilson *B*-value (Å^2)	118	111
Ramachandran values (%)[e]	96.6, 0.7	90.6, 3.3
R.m.s.d. bond (Å)	0.009	0.014
R.m.s.d. angle (deg.)	1.9	2.5
PDB ID	5CJS	5CJQ

[a] Parentheses denote outer-shell statistics.

[b] $R_{sym} = \sum_{hkl}\sum_i |I_{hkl,i} - \langle I_{hkl}\rangle| / \sum_{hkl}\sum_i I_{hkl,i}$ and $R_{pim} = \sum_{hkl}[1/(N-1)]^{1/2}\sum_i |I_{hkl,i} - \langle I_{hkl}\rangle| / \sum_{hkl}\sum_i I_{hkl,i}$, where $I_{hkl,i}$ is the scaled intensity of the ith measurement of reflection h, k, l, $\langle I_{hkl}\rangle$ is the average intensity for that reflection, and N is the redundancy. $R_{pim} = \Sigma_{hkl}\,(1/(n-1))^{1/2}\,\Sigma_i\,|\,I_{hkl,i} - \langle I_{hkl}\rangle\,|\,/\,\Sigma_{hkl}\,\Sigma_i\,I_{hkl,i}$, where n is the redundancy

[c] $R_{cryst} = \sum_{hkl}|F_o - F_c| / \sum_{hkl}|F_o|$, where F_o and F_c are the observed and calculated structure factors.

[d] R_{free} was calculated as for R_{cryst}, but on 5% of data excluded before refinement.

[e] The values are percentage of residues in the favored and outliers regions analyzed by MolProbity.

Table S2. Sequence comparison of mini-HA #4900 with some influenza HAs[a]

```
                                                  1         11        20        30
mini-HA_#4900                     MK-----VKLLVLLCTFTATY----ADTICIGYHANNSTDTVDTVLEKNV
A/California/04/2009[H1N1]        MK-----AILVVLLYTFATAN----ADTLCIGYHANNSTDTVDTVLEKNV
A/Brisbane/59/2007[H1N1]          MK-----VKLLVLLCTFTATY----ADTICIGYHANNSTDTVDTVLEKNV
A/New Caledonia/20/1999[H1N1]     MK-----AKLLVLLCTFTATY----ADTICIGYHANNSTDTVDTVLEKNV
A/Puerto Rico/8/1934[H1N1]        MK-----ANLLVLLCALAAAD----ADTICIGYHANNSTDTVDTVLEKNV
A/Vietnam/1203/2004[H5N1]         ME------KIVLLFAIVSLVK----SDQICIGYHANNSTEQVDTIMEKNV
A/Hong Kong/1073/1999[H9N2]       ME---TISLITILLVVTASN-----ADKICIGHQSTNSTETVDTLTETNV
A/Wisconsin/67/2005[H3N2]         MKTIIALSYILCLVFAQKLPGNDNSTATLCLGHHAVPNGTIVKTITNDQI
A/Brisbane/10/2007[H3N2]          MKTIIALSYILCLVFTQKLPGNDNSTATLCLGHHAVPNGTIVKTITNDQI
A/Texas/50/2012[H3N2]             MKTIIALSYILCLVFAQKLPGNDNSTATLCLGHHAVPNGTIVKTITNDRI
A/Netherlands/219/03[H7N7]        MN-----TQILVFALVASIPTN---ADKICLGHHAVSNGTKVNTLTERGV

                                      40        307           320           329
mini-HA_#4900                     TVTHSVNLLENGGGGKYVCSAKLRMVTGLRNKPSKQ----SQ
A/California/04/2009[H1N1]        TVTHSVNLLEDKHNGKYVKSTKLRLATGLRNIPSIQ----SR
A/Brisbane/59/2007[H1N1]          TVTHSVNLLENSHNGKYVRSAKLRMVTGLRNIPSIQ----SQ
A/New Caledonia/20/1999[H1N1]     TVTHSVNLLEDSHNGKYVRSAKLRMVTGLRNIPSIQ----SR
A/Puerto Rico/8/1934[H1N1]        TVTHSVNLLEDSHNGKYVRSAKLRMVTGLRNIPSIQ----SR
A/Vietnam/1203/2004[H5N1]         TVTHAQDILEKKHNGKYVKSNRLVLATGLRNSPQRERRRKKR
A/Hong Kong/1073/1999[H9N2]       PVTHAKELLHTEHNGMYVRVNSLKLAVGLRNVPARS----SR
A/Wisconsin/67/2005[H3N2]         EVTNATELVQSSSTGGYVKQNTLKLATGMRNVPEK----QTQ
A/Brisbane/10/2007[H3N2]          EVTNATELVQSSSTGEYVKQNTLKLATGMRNVPEK----QTR
A/Texas/50/2012[H3N2]             EVTNATELVQNSSIGEYVKQSTLKLATGMRNVPEK----QTR
A/Netherlands/219/03[H7N7]        EVVNATETVERTNVPRYVKQESLLLATGMKNVPEIPKR-RRR

                                  1         10        20        30        40        50
mini-HA_#4900                     GLFGAIAGFTEGGWTGMVDGWYGYHHQNEQGSGYAADQKSTQNAINGITN
A/California/04/2009[H1N1]        GLFGAIAGFIEGGWTGMVDGWYGYHHQNEQGSGYAADLKSTQNAIDEITN
A/Brisbane/59/2007[H1N1]          GLFGAIAGFIEGGWTGMVDGWYGYHHQNEQGSGYAADQKSTQNAINGITN
A/New Caledonia/20/1999[H1N1]     GLFGAIAGFIEGGWTGMVDGWYGYHHQNEQGSGYAADQKSTQNAINGITN
A/Puerto Rico/8/1934[H1N1]        GLFGAIAGFIEGGWTGMIDGWYGYHHQNEQGSGYAADQKSTQNAINGITN
A/Vietnam/1203/2004[H5N1]         GLFGAIAGFIEGGWQGMVDGWYGYHHSNEQGSGYAADKESTQKAIDGVTN
A/Hong Kong/1073/1999[H9N2]       GLFGAIAGFIEGGWPGLVAGWYGFQHSNDQGVGMAADRDSTQKAIDKITS
A/Wisconsin/67/2005[H3N2]         GIFGAIAGFIENGWEGMVDGWYGFRHQNSEGIGQAADLKSTQAAINQING
A/Brisbane/10/2007[H3N2]          GIFGAIAGFIENGWEGMVDGWYGFRHQNSEGIGQAADLKSTQAAIDQING
A/Texas/50/2012[H3N2]             GIFGAIAGFIENGWEGMVDGWYGFRHQNSEGRGQAADLKSTQAAIDQING
A/Netherlands/219/03[H7N7]        GLFGAIAGFIENGWEGLIDGWYGFRHQNAQGEGTAADYKSTQSAIDQITG

                                            60        70        80        90        100
mini-HA_#4900                     KVNSVIEKMNTQYTAIGCEYNKSERCMKQIEDKIEEIESKIWCYNAELLV
A/California/04/2009[H1N1]        KVNSVIEKMNTQFTAVGKEFNHLEKRIENLNKKVDDGFLDIWTYNAELLV
A/Brisbane/59/2007[H1N1]          KVNSVIEKMNTQFTAVGKEFNKLERRMENLNKKVDDGFIDIWTYNAELLV
A/New Caledonia/20/1999[H1N1]     KVNSVIEKMNTQFTAVGKEFNKLERRMENLNKKVDDGFLDIWTYNAELLV
A/Puerto Rico/8/1934[H1N1]        KVNTVIEKMNIQFTAVGKEFNKLEKRMENLNKKVDDGFLDIWTYNAELLV
A/Vietnam/1203/2004[H5N1]         KVNSIIDKMNTQFEAVGREFNNLERRIENLNKKMEDGFLDVWTYNAELLV
A/Hong Kong/1073/1999[H9N2]       KVNNIVDKMNKQYEIIDHEFSEVETRLNMINNKIDDQIQDVWAYNAELLV
A/Wisconsin/67/2005[H3N2]         KLNRLIGKTNEKFHQIEKEFSEVEGRIQDLEKYVEDTKIDLWSYNAELLV
A/Brisbane/10/2007[H3N2]          KLNRLIGKTNEKFHQIEKEFSEVEGRIQDLEKYVEDTKIDLWSYNAELLV
A/Texas/50/2012[H3N2]             KLNRLIGKTNEKFHQIEKEFSEVEGRIQDLEKYVEDTKIDLWSYNAELLV
A/Netherlands/219/03[H7N7]        KLNRLIEKTNQQFELIDNEFTEVERQIGNVINWTRDSMTEVWSYNAELLV

                                          110       120       130       140       150
mini-HA_#4900                     LLENERTLDFHDSNVKNLYEKVKSQLKNNAKEIGNGCFEFYHKCNDECME
A/California/04/2009[H1N1]        LLENERTLDYHDSNVKNLYEKVRSQLKNNAKEIGNGCFEFYHKCDNTCME
A/Brisbane/59/2007[H1N1]          LLENERTLDFHDSNVKNLYEKVKSQLKNNAKEIGNGCFEFYHKCNDECME
A/New Caledonia/20/1999[H1N1]     LLENERTLDFHDSNVKNLYEKVKSQLKNNAKEIGNGCFEFYHKCNNECME
A/Puerto Rico/8/1934[H1N1]        LLENERTLDFHDSNVKNLYEKVKSQLKNNAKEIGNGCFEFYHKCDNECME
A/Vietnam/1203/2004[H5N1]         LMENERTLDFHDSNVKNLYDKVRLQLRDNAKELGNGCFEFYHKCDNECME
A/Hong Kong/1073/1999[H9N2]       LLENQKTLDEHDANVNNLYNKVKRALGSNAMEDGKGCFELYHKCDDQCME
A/Wisconsin/67/2005[H3N2]         ALENQHTIDLTDSEMNKLFERTKKQLRENAEDMGNGCFKIYHKCDNACIG
A/Brisbane/10/2007[H3N2]          ALENQHTIDLTDSEMNKLFEKTKKQLRENAEDMGNGCFKIYHKCDNACIG
A/Texas/50/2012[H3N2]             ALENQHTIDLTDSEMNKLFEKTKKQLRENAEDMGNGCFKIYHKCDNACIG
A/Netherlands/219/03[H7N7]        AMENQHTIDLADSEMNKLYERVKRQLRENAEEDGTGCFEIFHKCDDDCMA

                                          160       170       180       190
mini-HA_#4900                     SVKNGTYDYPKYSEESKLNREKIDGVKLESMGVYQIEGRHHHHHHH
A/California/04/2009[H1N1]        SVKNGTYDYPKYSEEAKLNREEIDGVKLESTRIYQILAIYSTVASS
A/Brisbane/59/2007[H1N1]          SVKNGTYDYPKYSEESKLNREKIDGVKLESMGVYQILAIYSTVASS
```

A/New Caledonia/20/1999[H1N1]	SVKNGTYDYPKYSEESKLNREKIDGVKLESMGVYQILAIYSTVASS
A/Puerto Rico/8/1934[H1N1]	SVRNGTYDYPKYSEESKLNREKVDGVKLESMGIYQILAIYSTVASS
A/Vietnam/1203/2004[H5N1]	SVRNGTYDYPQYSEEARLKREEISGVKLESIGIYQILSIYSTVASS
A/Hong Kong/1073/1999[H9N2]	TIRNGTYNRRKYREESRLERQKIEGVKLESEGTYKILTIYSTVASS
A/Wisconsin/67/2005[H3N2]	SIRNGTYDHDVYRDEALNNRFQIKGVELKS-GYKDWILWISFAISC
A/Brisbane/10/2007[H3N2]	SIRNGTYDHDVYRDEALNNRFQIKGVELKS-GYKDWILWISFAISC
A/Texas/50/2012[H3N2]	SIRNGTYDHDVYRDEALNNRFQIKGVELKS-GYKDWILWISFAISC
A/Netherlands/219/03[H7N7]	SIRNNTYDHSKYREEAIQNRIQIDPVKLSS-GYKDVILWFSFGASC

[a] The H3 numbering is used. The solvent accessible residues (not totally buried) as indicated in the crystal structure of mini-HA #4900 in its complex with CR9114 and H1 HA structure from A/California/04/2009 (PDB ID 4M4Y) are highlighted in cyan. The missing residues in both structures are highlighted in yellow. The residue solvent accessible area was evaluated with program MS (65).
The CR9114 epitope residues (*3*) on mini-HA #4900 by group 1 and 2 influenza A viruses are highlighted in red letters.

Table S3. Comparison of solvent accessible area of CR9114 epitope residues in mini-HA #4900 and Cali04 H1[a]

#4900		Cali04 H1	
Residue	Accessible area (Å^2)	Residue	Accessible area (Å^2)
HA1 His38	71	HA1 His38	57
HA1 Val40	44	HA1 Val40	40
HA1 Asn41	85	HA1 Asn41	56
HA2 Val18	73	HA2 Val18	76
HA2 Asp19	80	HA2 Asp19	68
HA2 Gly20	16	HA2 Gly20	18
HA2 Trp21	39	HA2 Trp21	36
HA2 Ala36	25	HA2 Ala36	15
HA2 Gln38	92	HA2 Leu38	92
HA2 Thr41	21	HA2 Thr41	18
HA2 Gln42	65	HA2 Gln42	59
HA2 Ile45	53	HA2 Ile45	50
HA2 Asn46	67	HA2 Asp46	59
HA2 Ile48	17	HA2 Ile48	11
HA2 Thr49	59	HA2 Thr49	58
HA2 Val52	31	HA2 Val52	25
HA2 Ile56	65	HA2 Ile56	40

[a] The residue solvent accessible area was evaluated with program MS (65).

Only two residues differ for the antibody CR9114 epitope residues (*3*) in mini-HA #4900 (based on A/Brisbane/59/07) and Cali04 H1 (HA from A/California/04/2009 (H1N1), PDB ID 4M4Y).